(ANPA Conference 2024)
ISSN: 2392-473X(Print), 2738-9537 (Online)

Research Article ©Nepal Physical Society
DOI:https://doi.org/10.3126/jnphyssoc.v10i1.73389

Seasonal Tropopause Dynamics Over Nepal from 2022 to 2023: Insights from GNSS-RO Observations

Madhu Sudan Paudel,[1, 2, a)] Basu Dev Ghimire,[3, b)] and Narayan Prasad Chapagain[4, c)]

[1)]*Department of Physics, Tri-Chandra Multiple Campus, TU, Nepal*
[2)]*Central Department of Physics, IoST, TU, Nepal.*
[3)]*St.Xavier's College, TU, Maitighar, Kathmandu*
[4)]*Amrit Campus, TU, Nepal*

[a)]*Corresponding author: madhu.paudel@trc.tu.edu.np, mspaudel27@gmail.com*
[b)]*Electronic mail: basudev@sxc.edu.np*
[c)]*Electronic mail: npchapagain@gmail.com*

Abstract. Global Navigation and Satellite System-Radio Occultation (GNSS-RO) is the robust method for monitoring the Earth's atmosphere utilizing the refracted GNSS radio signal. Constellation Observation System for Meteorology, Ionosphere and Climate-2 (COSMIC-2) is one of the GNSS-RO satellite missions providing the bunch of information, which enables us to explore the characteristics of Earth's atmosphere. It can provide the vertical profile of the atmospheric thermodynamic variable globally with better resolution. The GNSS-RO data features the long-term stability, continuous in all types of weather condition along with very high precision and accuracy. In this work, we are going to study the tropopause dynamics within the periphery of the Nepal, from longitude: 79°E to 89°E and latitude: 26°N to 31°N, using the data from COSMIC-2 mission from April 01, 2022 to March 30, 2023, by dividing into four seasons; March-April-May (MAM), June-July-August (JJA), September-October-November (SON) and December-January-February (DJF). For data extraction, we use the *netCDF4* and *Pandas* and for the visualization and statistical analysis, we use the *Matplotlib*, *Basemap*, *Scipy*, *Scikit-learn*, libraries of the Python. The tropopuse height (TRH) and tropopause temperature (TRT) is studied from vertical profile of the temperature using World Meteorological Organization (WMO) and Cold Point (CP) method. The TRH is found maximum in JJA and minimum in MAM in WMO method. In CP method, TRH is obtained maximum in MAM and minimum in SON. The WMO method is found best to explain the variation of the TRH along the latitude. However, the CP method is more accurate to the reference data from COSMIC2 compare to the WMO method.

Keywords: GNSS-RO, COSMIC-2, Tropopause-dynamics, Nepal, WMO1957.

Received: August 25, 2024; **Revised**: December 15, 2024; **Accepted**: December 23, 2024

INTRODUCTION

The Global Navigation Satellite System (GNSS) is the constellation of the satellites in the medium earth orbit (MEO) for the continuous observation of Earth to provide accurate position and velocity. When the radio signal from GNSS travels from satellite system to the receiver at ground station, it passes through the ionosphere and troposphere of the Earth. The behaviour of the GNSS signal to the ionosphere and troposphere is slightly different because the ionospheric is a dispersive medium and troposphere is the non-dispersive medium. Both mediums introduce the error to the pseudorange of the signal. These errors introduced by ionospheric and troposphere to the pseudorange are very important to estimate the properties of these mediums.

The density of the air continuously decreases as we move above the surface of the Earth. Due to the density variation, the GNSS signal gets refracted as it enters the atmosphere, the process of bending the GNSS signal depends on the density gradient. This refraction of an electromagnetic (EM) signal in radio frequency (RF) in the planetary atmosphere is often pronounced as radio occultation. The RF signal from the GNSS satellite refracted from the Earth's atmosphere can be received by a low earth orbiting (LEO) satellite, which can be used to ex-

tract atmospheric properties, such as; temperature, pressure, etc. This is known as the GNSS Radio Occultation (GNSS-RO).

GNSS-RO and COSMIC2

GNSS-RO is the limb-sounding method for the atmospheric observation. The GNSS satellite constellation in MEO, along with the LEO satellite to receive the refracted GNSS signal, together constitute the GNSS-RO system. The relative change in position between GNSS satellites and LEO satellites facilitates the inspection of the atmospheric layers vertically. GNSS-RO has wide applications in scientific research, including the fields of meteorology, space weather, physics of earth science, oceanography, etc. In its initial days, it was used for the study of the atmosphere of the other planets, like Mars, Venus, Saturn, Uranus, Neptune, and their natural satellites. Global Positioning System/Meteorology (GPS/MET) is the first mission started in 1995 focussing on the atmosphere of the Earth [1].

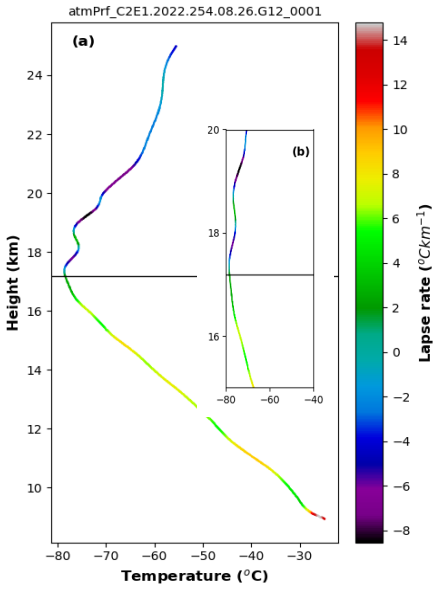

FIGURE 1. A typical vertical profile of the temperature at DOY of 254 of 2022, horizontal line represents TRH from WMO and color bar represents the lapse rate. An extended view can be seen in figure (b) near tropopause.

Constellation Observing System for Meteorology, Ionosphere, and Climate (COSMIC), also known as the Formosa Satellite Mission 3 (FORMOSAT-3), is the another GNSS-RO mission launched in 2006 by U.S. agencies and Taiwan, which can provide improved spatial coverage in comparison to other earlier GNSS-RO missions

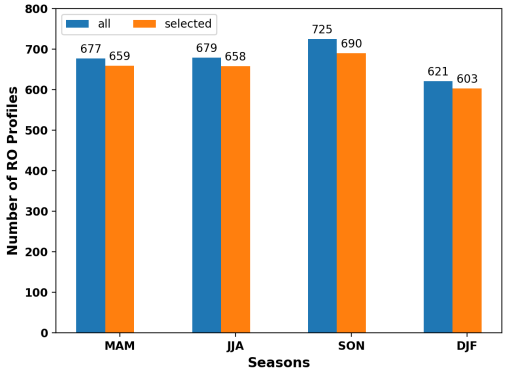

FIGURE 2. The figure shows the histogram of the number of the total GNSS RO profile and selected RO profile in the different seasons.

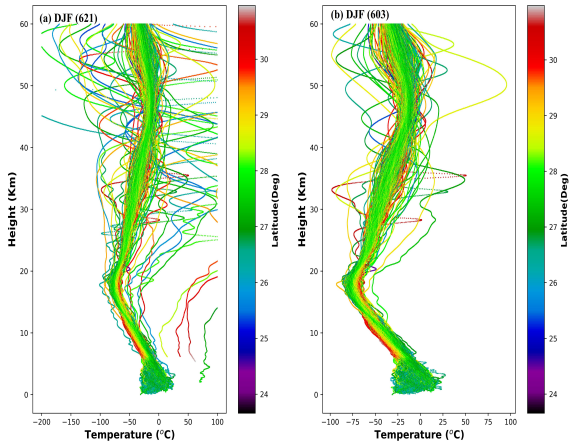

FIGURE 3. Vertical profile of the temperature for (a) total and (b) selected GNSS RO profile in DJF. The GNSS RO profile having temperature range more than 200°C are removed from total profile to get selected profile.

[2]. After its successful operation, the organisers lunched the COSMIC-2/FORMOSAT-7 mission on 2019. It can provide more than 5000 atmospheric profiles per day, covering the entire longitude and latitude from 45°S to 45°N.

Troposphere and Tropopause

Troposphere is the lowermost part of the atmosphere connected with the surface of the Earth physically and chemically. Its constituents can be classified into dry and wet components with the former covering 90 % and later 10%. The dry component is more stable and effects can be predictable, and the wet component is very unstable and can't be predicted due to the presence of most fluctuating com-

ponent, water vapour. The concentration of the water vapour dominates in the lower troposphere, below 3 km, and as the altitude increases, the dry components predominate over wet components. The variation of temperature with altitude is measured in terms of lapse rate (LR) ($-\frac{dT}{dz}$), in the unit ($^{\circ}$Ckm^{-1}), which decreases with increase in altitude and becomes more or less constant at the boundary of troposphere and stratosphere. The boundary layer, also called tropopause, is also defined on the basis of LR variation; the definition of tropopause defined by the general assembly of the World Meteorological Organisation 1957 (WMO1957), given in the following section. The tropopause height (TRH) and tropopause temperature (TRT) vary along with the latitude. The mean value of TRH is $\sim$17 km in the tropical region with TRT $\sim$ -80°C and for the extra-tropical region, the mean value of TRH decreases to $\sim$ 10 km [3].
In this paper, we have presented the result of the variation of TRH and TRT in the periphery of the Nepal by using the data from COSMIC2 satellite. The tropopause dynamics at different seasons according to the data from April 2022 to March 2023 is presented and the result obtained is compared with the reference value obtained from COSMIC2.

DATA AND METHOD

Source of Data

The GNSS-RO data from the COSMIC-2 mission is taken from the website of Taiwan Space Agency (`https://data.cosmic.ucar.edu/gnss-ro/cosmic2/nrt/`), available publicly. There are large variety of data for ionosphere, atmosphere, climate, etc., in which we have used the dry atmospheric profile, indicated by label 2. There are $\sim$ 5000 RO profiles for each day. The data are initially available in zip format as *.tar* file, after unziping *netCDF4* file with format *.0001_nc* is obtained. Each file consists of the following parameters;

```
Lat, Lon, MSL_alt, Ref, Azim,
Pres, Temp, Bend_ang1, Bend_ang2,
Bend_ang, Impact_height, Ref_L1,
Bend_ang_stdv, Bend_ang_conf, ies,
hes, wes, OL_par, OL_ipar,
OL_vec1, OL_vec2, OL_vec3, OL_vec4
```

For the estimation of TRH and TRT, we have used only longitude (Lon), latitude (Lat), mean sea level altitude (MSL_alt), and temperature (Temp).
The coverage of the COSMIC-2 data is from latitude 45°S to 45 $^{\circ}$N and it encompasses all the longitudes, from 0° to 360 $^{\circ}$. The latitude and longitude range for Nepal are; 26.35°N to 30.45°N and 80.06°E to 88.20°E. The tropopause dynamics depends on the meteorological parameter of periphery of the selected region. Due to this reason RO profile is selected half degree beyond the boundary of Nepal, which is; 26°N to 31°N latitude and 79°E to 89°E longitude. The spatial variation of the RO profile also shows this types of variation. The latitude of Nepal belongs in such a region in which the TRH shows wide variation, being a sub-tropical region.
The one year data is divided into four seasons; the name of the seasons are selected as follows; March, April, May by MAM, June, July, August by JJA, September, October, November by SON and December, January and February by DJF following the paper [4].

Methods

Tropopause Estimation

In this paper, we have used two different method to estimate the height of the tropopause. Which are given below;

Cold Point Method
The temperature goes on decreasing as we move above in the troposphere. When the temperature decrease to it's minimum value then it becomes constant for few altitude and then again starts to increase. The point nearby the tropopause at which the temperature becomes minimum is called cold point (CP). In the lower part of the troposphere, below 10 km, multiple inversion point can be seen, which creates the multiple local CP. The World Meteorological Organization (WMO) defines the cutoff height at given latitudes according to the following equation:

$$H_{cut}(lat) = 7.5 + 2.5cos(2 \times lat) \quad (1)$$

This value of the height given by equation (1) is the minimum height that is actually considered as the minimum cut-off height, at a given latitude. If there is a profile for which the penetration height is less than the cut off height then it is replaced by the cut-off height for the calculation of the height and temperature at CP. This criterion is used to avoid the accidental occurrence of the cold point at the lower part of the troposphere.
World Meteorological Organization 1957: WMO 1957
The tropopause can be defined based on the variation of the temperature, chemical composition, dynamical process, etc. The LR method of determination of the tropopause is based on the variation of the temperature. The World Meteorological Organization (WMO) has given a very clear definition about the tropopause based on the variation of LR along the altitude. The definition is called the WMO criteria. According to WMO (1957) [5] the tropopause is defined as the lowest altitude

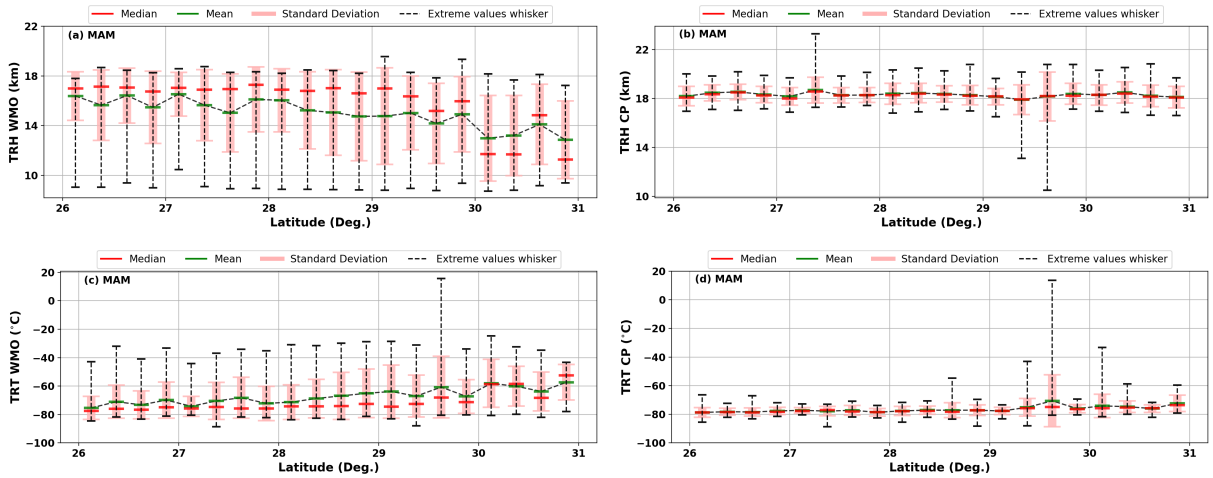

FIGURE 4. Variation mean (green line), median (red line), standard deviation (red box) and extreme outlier (dotted line) of TRH [(a) and (b)] and TRT[(c) and (d)] in MAM along the latitude can be seen in the figure. The data is binned for 0.25° latitude.

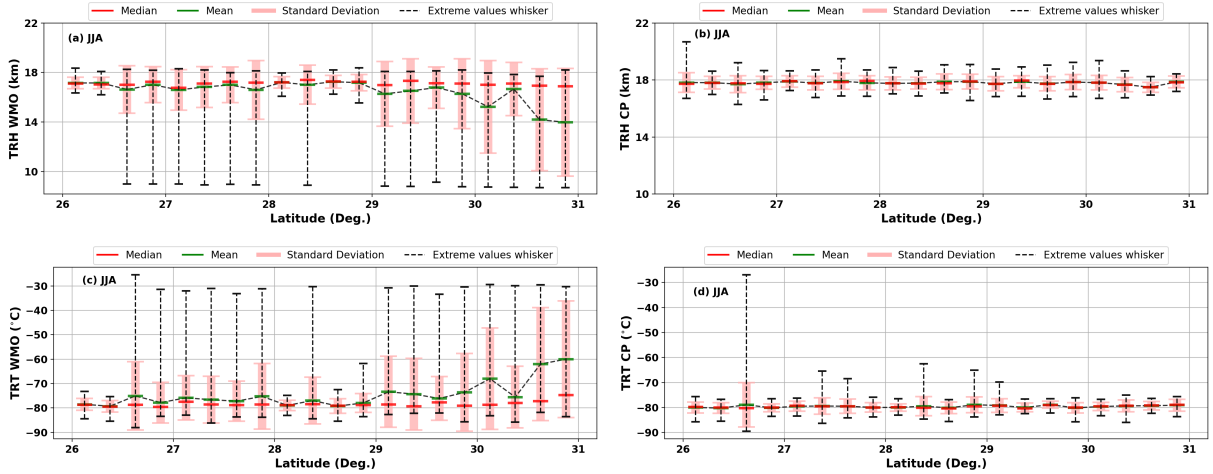

FIGURE 5. Variation mean (green line), median (red line), standard deviation (red box) and extreme outlier (dotted line) of TRH [(a) and (b)] and TRT[(c) and (d)] in JJA along the latitude can be seen in the figure. The data is binned for 0.25° latitude.

at which the LR decreases to 2 °C km^{-1} or less and above this altitude, upto next 2 km the average LR is less than or equal to 2 °C km^{-1}. The second condition ensures that no RO profile accidentally considers a shallow stable layer in troposphere as the tropopause. [5]

Cubic Spline Interpolation

The vertical resolution of the COSMIC-2 data is very good, $\sim$ 20 m, however we are seeking the more vertical resolution. The CubicSpline interpolation [6] is used for this purpose. We use *scipy* library in python for *Cubic-Spline* interpolation, which takes two dimensional variable. In our work, we have used four variables; altitude, temperature, latitude and longitude. Keeping the altitude data array same, we interpolate for temperature, latitude and longitude again and again. The minimum altitude is chosen at least above the cut-off height given by equation (1) at given latitude. After interpolating, we get the data set of height with 10 m vertical resolution.

Data Pre-processing

In this work, we are interested to study the variation of TRH and TRT by using the data of vertical profile of the

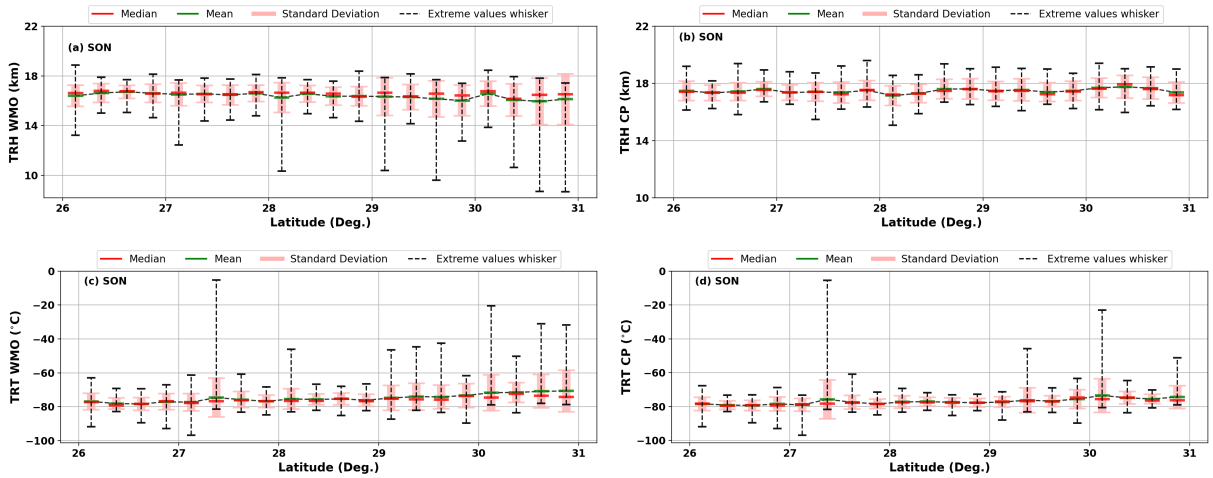

FIGURE 6. Variation mean (green line), median (red line), standard deviation (red box) and extreme outlier (dotted line) of TRH [(a) and (b)] and TRT[(c) and (d)] in SON along the latitude can be seen in the figure. The data is binned for 0.25° latitude.

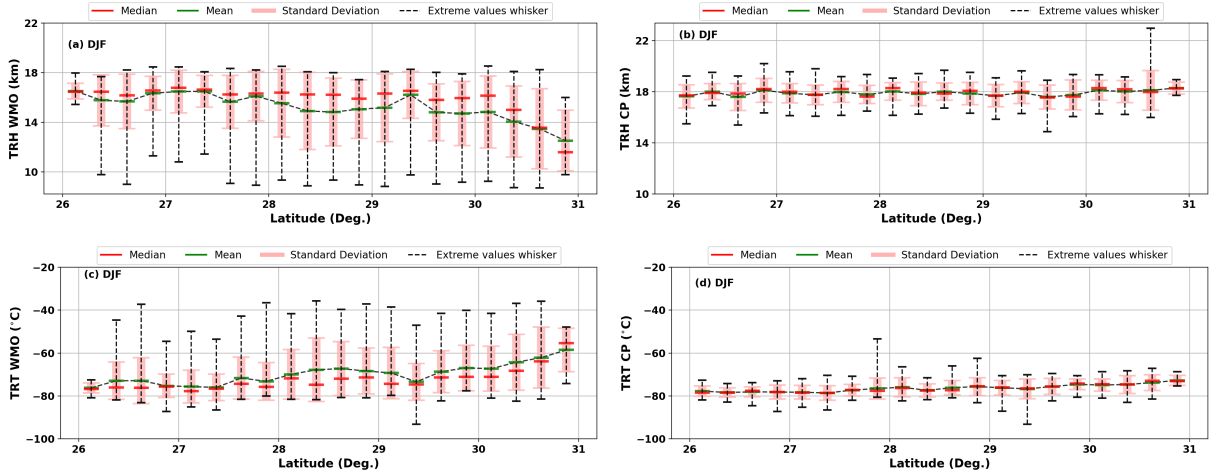

FIGURE 7. Variation mean (green line), median (red line), standard deviation (red box) and extreme outlier (dotted line) of TRH [(a) and (b)] and TRT[(c) and (d)] in DJF along the latitude can be seen in the figure. The data is binned for 0.25° latitude.

temperature from each GNSS-RO profile. A typical vertical profile can be seen as given in FIGURE 1. The temperature first decrease as height increases. At a point, called tropopause, the temperature is fairly constant as defined by the WMO 1957 [5]. Above the tropopause, the temperature starts to increase. In this figure, the temperature variation can be seen ~ 100°C, and can vary slightly more or less. The variation of LR can be seen in color bar. To make the variation of LR more clear, a zoom view of subplot is also seen in FIGURE 1(b). There are few GNSS RO profiles in COSMIC2 data for which the the variation of the temperature is unusually large. To exclude these types of the profiles, we applied three Quality Control (QC) process. We exclude those GNSS RO profile; (1) which starts above 10 km height, (2) which ends below 40 km, and (3) which have temperature range more than 200°C. The total and selected GNSS RO profiles in different seasons before and after applying these QCs can be seen in the bar plot in FIGURE 2. The vertical profile of the temperature of all and selected profiles in DJF season can be seen in FIGURE 3. In FIGURE 3(a) the many vertical profiles can be seen with huge random fluctuations in temperature. After removing those vertical profiles having temperature range more than 200°C, a clean set of vertical profile is obtained in FIGURE 3(b). The color bar in both figure represents the latitude.

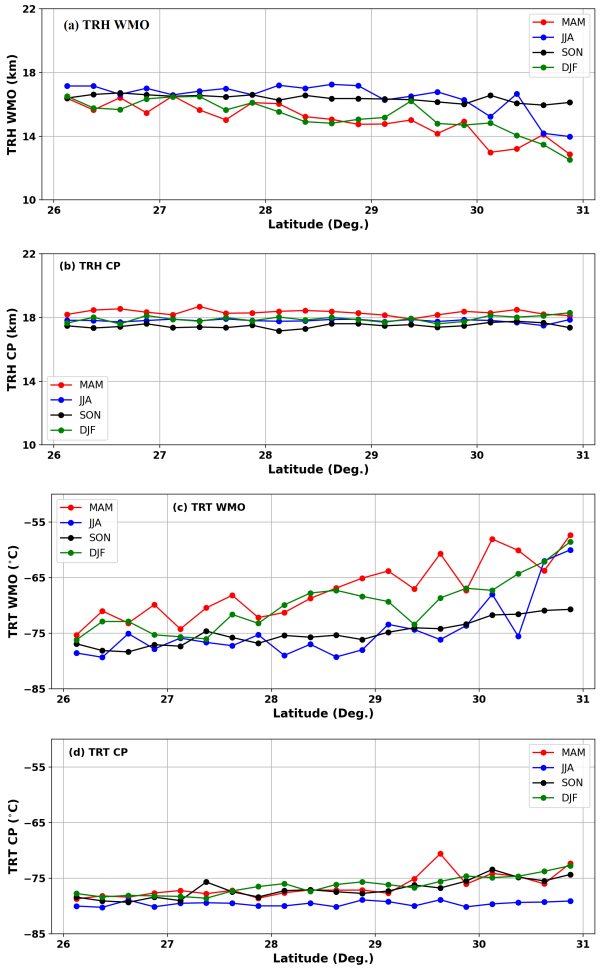

FIGURE 8. Comparison of mean value of TRH and TRT along the latitude in different seasons.

RESULTS AND DISCUSSION

The variation of the TRH (a and b) and TRT (c and d) for both WMO (a and c) and CP (b and d) method is presented in the FIGURE 4 for MAM, FIGURE 5 for JJA, FIGURE 6 for SON and FIGURE 7 for DJF. In each figure, the variation of mean, median, standard and extreme outliers can be seen. The data is binned along the latitude at the difference of 0.25 ° latitude.

In all seasons, the variation trends of the TRH and TRT along the latitude is more or less similar, however, there is some differences in the mean and median value. The variation is fairly constant in CP method compare to the WMO method. Also, the standard deviation and extreme outliers are also small in CP method compare to the WMO method. In many research, [7, 8] it is reported that there is decrease in TRH as the latitude increases. This trends can be seen only in WMO method. Moreover, the increase of the TRT is observed along with the increase in latitude

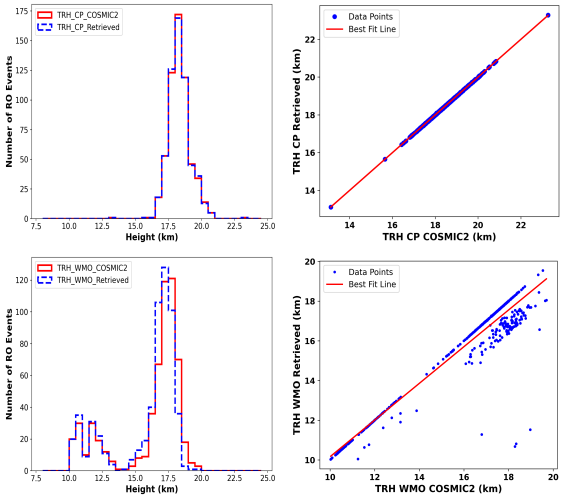

FIGURE 9. Histogram (left) and scatter plot (right) between retrieved and reference (COSMIC2) TRH by CP (top panel) and WMO (bottom panel) method MAM.

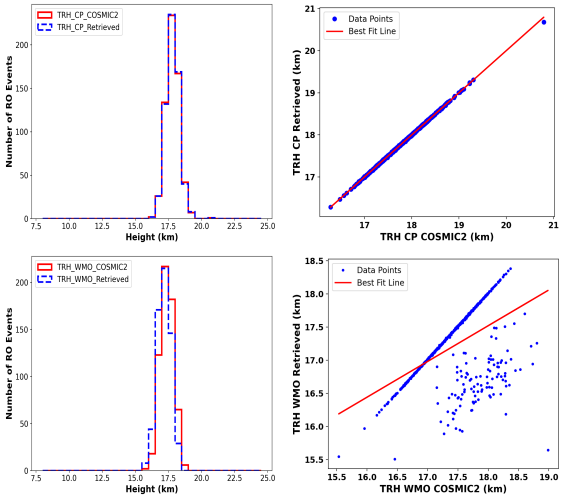

FIGURE 10. Histogram (left) and scatter plot (right) between retrieved and reference (COSMIC2) TRH by CP (top panel) and WMO (bottom panel) method in JJA.

in WMO method. The CP method fails to explain the variation of the TRH and TRT along the latitude in all seasons.

COMPARISON OF TRH AND TRT FOR DIFFERENT SEASONS

The mean value of variation of TRH and TRT along the latitude is presented in FIGURE 8. In FIGURE 8(a), it is seen that the TRH value is higher in the season JJA and

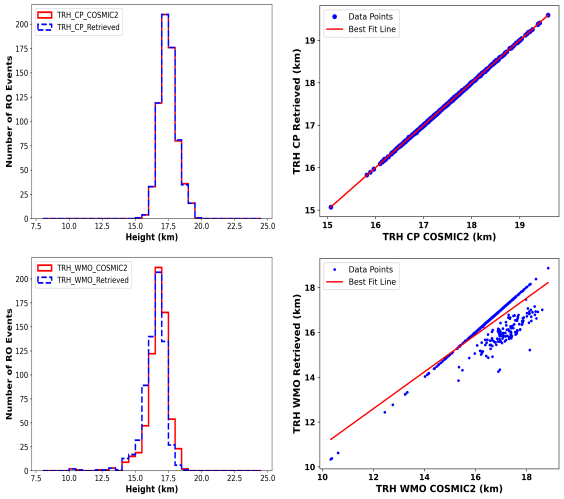

FIGURE 11. Histogram (left) and scatter plot (right) between retrieved and reference (COSMIC2) TRH by CP (top panel) and WMO (bottom panel) method in SON.

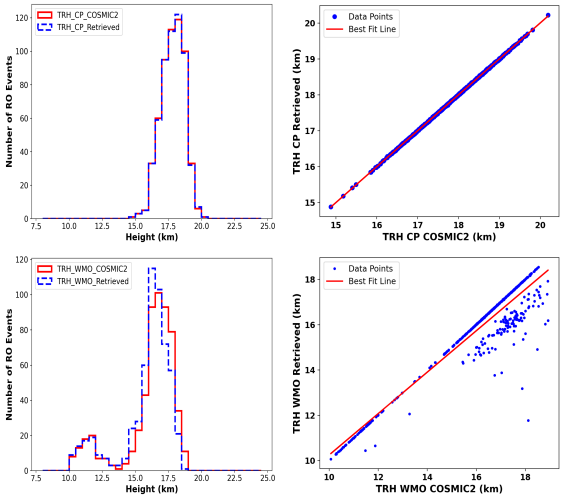

FIGURE 12. Histogram (left) and scatter plot (right) between retrieved and reference (COSMIC2) TRH by CP (top panel) and WMO (bottom panel) method in DJF.

lower in MAM in WMO method. In SON and DJF, the TRH value lies in between. The value is most consistent in SON. In all other seasons, the value decreases as the value of latitude increases. This is a very well expected result. In FIGURE 8(b), TRH value by CP method can be seen, TRH is highest in MAM and lowest in SON, in DJF and JJA the TRH value lies in between. The value of TRH is most consistent in JJA and SON. In other seasons, the TRH value is fluctuating but neither increasing nor decreasing with the latitude as in WMO method. In both method, the TRH in SON is found most consistent. The variation in TRH is more in WMO method.

In FIGURE 8(c), the variation of the TRT by WMO method in different seasons can be seen. The highest value of TRT can be seen in DJF and lowest value in JJA. In SON, the TRT value is most consistent. Moreover, the TRT value is increasing with the increase in latitude in all seasons. The variation of TRT by CP method in all seasons can be seen in FIGURE 8(d). The figure shows highest value in DJF and lowest in JJA season. In MAM, the data is most fluctuating and in JJA it is most consistent. The overall trends shows the increase in TRT for increasing latitude. But the increasing rate is low compare to the WMO method.

COMPARISON WITH REFERENCE (COSMIC2) RESULT

The retrieved value of TRH by both WMO and CP method is compared with the reference value from COSMIC2 satellite data. The reference value of the TRH is available on each atmospheric profile data. We implement two ways to compare the retrieved and reference data; histogram and scatter diagram. We have compared the result for each four seasons. The mean value of TRH with standard error (SE) and standard deviation (SD) for different seasons is presented in TABLE I. The mean value of TRH is maximum in JJA and minimum in MAM in WMO method but in CP method it is maximum in MAM and minimum in SON. The value of TRH is more consistent in all seasons in CP method compare to WMO. The value of SD shows that TRH is more scattered in MAM and least in JJA in both method. The comparison of the retrieved result with the reference result from COSMIC2 is presented in TABLE II. It can be seen that, bias is maximum in MAM and minimum in JJA in WMO method and maximum in SON and minimum in JJA in CP method. The root mean square error (RMSE) is also consistent with the SD in both CP and WMO method. The overall result shows that the bias is very less in CP method

TABLE I. Mean $\pm$ SE and SD of the TRH in CP and WMO method in both retrieve and reference data in each seasons.

Quantity	Data	Methods	Mean $\pm$ SE	SD
MAM	Retrieved	CP	$18.33 \pm 1.40 \times 10^{-3}$	0.83
		WMO	$15.82 \pm 4.23 \times 10^{-3}$	2.49
JJA	Retrieved	CP	$17.81 \pm 8.25 \times 10^{-4}$	0.51
		WMO	$17.18 \pm 4.01 \times 10^{-4}$	0.51
SON	Retrieved	CP	$17.47 \pm 9.74 \times 10^{-4}$	0.67
		WMO	$16.44 \pm 1.33 \times 10^{-3}$	0.90
DJF	Retrieved	CP	$17.84 \pm 1.50 \times 10^{-3}$	0.86
		WMO	$15.83 \pm 3.44 \times 10^{-3}$	1.90

TABLE II. Bias, RMSE value and r-value between the retrieved and reference calculation in both CP and WMO method.

Quantity	Methods	Bias(m)	RMSE(m)	r − value
MAM	CP	6.30	10.57	0.99
	WMO	296.39	764.99	0.95
JJA	CP	0.29	9.27	0.99
	WMO	199.74	486.17	0.53
SON	CP	6.58	10.72	0.99
	WMO	235.10	520.18	0.83
DJF	CP	1.30	7.89	0.99
	WMO	275.41	662.93	0.94

compare to WMO method. The r-value between the retrieved and reference data also shows same result. The histogram as well as the mean value of TRH in TABLE I both shows the TRH in CP method is sightly greater than WMO method in all seasons.

CONCLUSION

Following are the conclusions of this research work;

- We investigate the variation of the TRH and TRT over the Nepal from latitude 26°N to 31°N and found a clear decrease in TRH and increase in TRT with increase in latitude in WMO method. CP method fails to explain these variation with latitude.
- The value of TRH is found maximum in JJA and minimum in MAM, and in SON, it is most stable in WMO method. In CP method TRH is maximum in MAM and minimum in SON.
- The value of TRT is found maximum in JJA and minimum in MAM and most stable is in SON in WMO method. In CP method, it is found maximum in DJF and minimum in JJA.
- The CP method could not describe very well about the variation of the TRH and TRT along the latitude as does by WMO method, however the result obtained from CP method is close to the reference data provided by COSMIC2 in comparison to WMO method.

The study of tropopause dynamics for Nepal like region having complex terrain is very challenging task. We need to extend this work for long time data to get a proper conclusion. The result can be improve with the improvement in the QC process for selecting the appropriate GNSS RO profiles.

ACKNOWLEDGMENTS

We acknowledge the ANPA for providing the opportunity to present this in ANPA conference 2024. We also acknowledge to COSMIC2 data `https://www.cosmic.ucar.edu/what-we-do/cosmic-2/data` for for availability of the data for this work.

EDITORS' NOTE

This manuscript was submitted to the Association of Nepali Physicists in America (ANPA) Conference 2024 for publication in the special issue of the Journal of Nepal Physical Society.

REFERENCES

1. W. G. Melbourne, "Sounding the earth's atmosphere and ionosphere with gps," (1995).
2. R. A. Anthes, P. Bernhardt, Y. Chen, L. Cucurull, K. Dymond, D. Ector, S. Healy, S.-P. Ho, D. Hunt, Y.-H. Kuo, *et al.*, "The cosmic/formosat-3 mission: Early results," Bulletin of the American Meteorological Society **89**, 313–334 (2008).
3. J. M. Wallace and P. V. Hobbs, *Atmospheric science: an introductory survey*, Vol. 92 (Elsevier, 2006).
4. Z. Liu, W. Bai, Y. Sun, J. Xia, G. Tan, C. Cheng, Q. Du, X. Wang, D. Zhao, Y. Tian, *et al.*, "Comparison of ro tropopause height based on different tropopause determination methods," Atmospheric Measurement Techniques Discussions **2019**, 1–19 (2019).
5. World Meteorological Organization, "Meteorology – a three-dimensional science: Second session of the commission for aerology," Tech. Rep. Technical Paper No. 45 (World Meteorological Organization, Geneva, Switzerland, 1957) held from November 4-10, 1957.
6. E. Süli and D. F. Mayers, *An introduction to numerical analysis* (Cambridge university press, 2003).
7. Z. Liu, Y. Sun, W. Bai, J. Xia, G. Tan, C. Cheng, Q. Du, X. Wang, D. Zhao, Y. Tian, *et al.*, "Comparison of ro tropopause height based on different tropopause determination methods," Advances in Space Research **67**, 845–857 (2021).
8. T. Rieckh, B. Scherllin-Pirscher, F. Ladstädter, and U. Foelsche, "Characteristics of tropopause parameters as observed with gps radio occultation," Atmospheric Measurement Techniques **7**, 3947–3958 (2014).
9. S.-W. Son, N. F. Tandon, and L. M. Polvani, "The fine-scale structure of the global tropopause derived from cosmic gps radio occultation measurements," Journal of Geophysical Research: Atmospheres **116** (2011).
10. J. Wickert, C. Reigber, G. Beyerle, R. König, C. Marquardt, T. Schmidt, L. Grunwaldt, R. Galas, T. K. Meehan, W. G. Melbourne, *et al.*, "Atmosphere sounding by gps radio occultation: First results from champ," Geophysical research letters **28**, 3263–3266 (2001).
11. J. Wickert, G. Beyerle, R. König, S. Heise, L. Grunwaldt, G. Michalak, C. Reigber, and T. Schmidt, "Gps radio occultation with champ and grace: A first look at a new and promising satellite configuration for global atmospheric sounding," in *Annales Geophysicae*, Vol. 23 (Copernicus Publications Göttingen, Germany, 2005) pp. 653–658.

12. J. Wickert, G. Michalak, T. Schmidt, G. Beyerle, C.-Z. Cheng, S. B. Healy, S. Heise, C.-Y. Huang, N. Jakowski, W. Köhler, *et al.*, "Gps radio occultation: results from champ, grace and formosat-3/cosmic," Terrestrial Atmospheric and Oceanic Sciences **20**, 35–50 (2009).
13. S. Healy, J. Wickert, G. Michalak, T. Schmidt, and G. Beyerle, "Combined forecast impact of grace-a and champ gps radio occultation bending angle profiles," Atmospheric Science Letters **8**, 43–50 (2007).
14. T. Schmidt, S. Heise, J. Wickert, G. Beyerle, and C. Reigber, "Gps radio occultation with champ and sac-c: global monitoring of thermal tropopause parameters," Atmospheric Chemistry and Physics **5**, 1473–1488 (2005).
15. S. P. Parker, *McGraw-Hill concise encyclopedia of science & technology* (McGraw-Hill, 1984).
16. B. D. Santer, R. Sausen, T. Wigley, J. S. Boyle, K. AchutaRao, C. Doutriaux, J. Hansen, G. Meehl, E. Roeckner, R. Ruedy, *et al.*, "Behavior of tropopause height and atmospheric temperature in models, reanalyses, and observations: Decadal changes," Journal of Geophysical Research: Atmospheres **108**, ACL–1 (2003).
17. E. R. Kursinski, G. A. Hajj, S. S. Leroy, and B. Herman, "The gps radio occultation technique," Terrestrial Atmospheric and Oceanic Sciences **11**, 53–114 (2000).
18. E. K. Smith and S. Weintraub, "The constants in the equation for atmospheric refractive index at radio frequencies," Proceedings of the IRE **41**, 1035–1037 (1953).